Dispersions of Organically Modified Boehmite Particles and a Carboxylated Styrene–Butadiene Latix: A Simple Way to Nanocomposites

Zbigniew Florjańczyk,[1] Maciej Dębowski,[1] Andrzej Wolak,[1] Monika Malesa,[2] Justyna Płecha[1]

[1]*Faculty of Chemistry, Warsaw University of Technology, ul. Noakowskiego 3, 00-664 Warszawa, Poland*
[2]*Rubber Research Institute Stomil, ul. Harcerska 30, 05-820 Piastów, Poland*

Received 11 March 2006; revised 6 June 2006
DOI 10.1002/app.26013
Published online in Wiley InterScience (www.interscience.wiley.com).

ABSTRACT: Boehmite particles modified with organic ligands were prepared through the reaction of boehmite with acrylic acid or diethylphosphoric acid (formed in situ from triethyl phosphate). The chemical structures of these particles were determined, and it was shown that they formed stable aqueous dispersions with a particle size lower than 200 nm (average diameter = 40–100 nm, depending on the method of modification) for more than 90% of the population. These nanoparticle dispersions were mixed with carboxylated styrene–butadiene latex, and after water evaporation, homogeneous composites were obtained when the modifier concentration was in the range of 0.5–3 wt %. The mechanical properties of the composites were improved with respect to those of the unmodified rubber (tensile strength up to 200% and elongation at break up to 40%). The modifiers also improved some mechanical properties of rubbers cured with sulfur/N-cyclohexylbenzothiazole-2-sulfenamide/ZnO/stearic acid or ZnO/stearic acid systems. © 2007 Wiley Periodicals, Inc. J Appl Polym Sci 105: 80–88, 2007

Key words: boehmite; latices; nanocomposites; rubber

INTRODUCTION

The combination of organic polymers with inorganic nanofillers is regarded as a very promising method for tuning up the range of properties of polymeric materials. Many of the recent studies have been focused on thermoplastic composite materials containing delaminated smectic clays modified by organic compatibilizers. The most typical modification procedures include the swelling of inorganic materials via the cation-exchange process of inorganic cations located between negatively charged layers against hydrophobic organic onium cations.[1–7] There are also several examples of successful applications of a similar strategy to create exfoliated nanocomposite materials from ion-exchangeable, layered double hydroxides (LDH) such as synthetic hydrotalcites.[7,8] In the early 1990s, Barron and coworkers[9–14] disclosed a very simple synthetic method that allows the preparation of alumina nanoparticles decorated with carboxylate groups (carboxylate-alumoxanes) through the reaction of boehmite with carboxylic acids:

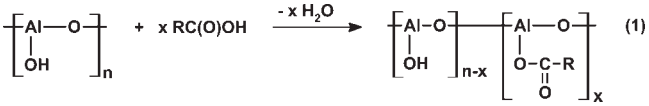

These materials can be prepared with a variety of functional groups, and this allows the alteration of the chemical properties of the carboxylate alumoxane surface and its covalent bonding with organic polymers.

In our laboratory, the possibility of the modification of boehmite with phosphoric acid diesters has been examined. The phosphoric acid diesters [$(RO)_2P(O)OH$] are structural analogues of carboxylic acids [RC(O)OH], but they display much stronger acidic properties. If the reaction of boehmite with phosphoric acid diesters is carried out long enough, total destruction of the boehmite core occurs. The final product of the process is chain-structured organic aluminum phosphate, the particles of which self-organize in macroscopic fibers:[15,16]

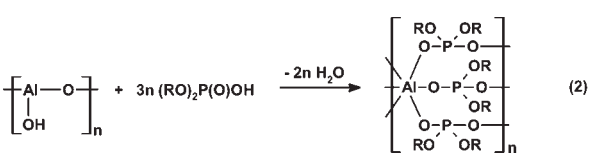

This reaction can be stopped, however, at the stage in which the product phase consists of nanospherical

This article is dedicated to the memory of Professor Marian Kryszewski.

Correspondence to: Z. Florjańczyk (evala@ch.pw.edu.pl).

Contract grant sponsor: State Committee for Scientific Research; contract grant numbers: PBZ-KBN-095/08/2003; 512/G/1020/0341.

particles with a boehmite core coated by organic aluminum phosphate:[16,17]

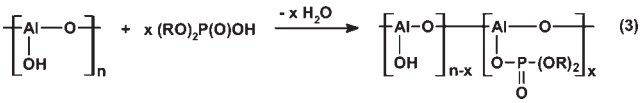

The products of the reaction of boehmite with some carboxylic acids or phosphoric acid diesters form stable aqueous nanodispersions. Such dispersions are convenient, applicable forms providing the possibility of homogeneously dispersing the nanoparticles in ceramic materials[12] and in water-soluble polymers.[16]

The modification of hydrophobic polymer latices and the obtaining of nanocomposites by coagulation or slow water evaporation seems to be another interesting application area. In this article, we present the preliminary results of research on such systems: boehmite particles were modified with small or large amounts of organic ligands and then dispersed in carboxylated styrene–butadiene latex (XSBL). On the basis of a set of optimization experiments (which are not described here), we selected two kinds of nanoparticles that easily formed stable dispersions in water. These included particles of A obtained in the reaction with diethyl phosphate [see eq. (3), where R = $-C_2H_5$ and $x = 0.09$] and particles of B containing acrylic acid segments [see eq. (1), where R = $-CH{=}CH_2$ and $x = 0.83$]. The main purpose of our work was the physicochemical characterization of these hybrid nanoparticles, both in the solid state and in a dispersion, and the determination of whether they could be applied to improve the properties of rubber before and after vulcanization.

EXPERIMENTAL

Materials

The starting materials for the synthesis were as follows: boehmite (ca. 75 wt % Al_2O_3; Catapal D Alumina, Condea–Vista Co., Houston, TX), triethyl phosphate (99%), acrylic acid (99%), and hydroquinone (99%) all purchased from Aldrich-Chemie GmbH, Steinheim, Germany; XSBL (48 wt % solids, LBSK 4148), (Dwory S.A.; Oświęcim, Poland), ZnO (pure) (Huta Oława; Poland), stearic acid (technical grade; Tefacid RG), (Tefac, Karslsham, Sweden), sulfur (pure) (Chempol; Warsaw, Poland), N-cyclohexylbenzothiazole-2-sulfenamide (CBS) (pure) Vulkacit, Bayer AG, Leverkusen, Germany). The listed materials were used as received without further purification, except for acrylic acid, which was redistilled under reduced pressure directly before use.

Preparation of the fillers

The synthesis of A was carried out according to the following procedure. Boehmite (2.0 g, 33.3 mmol) was dispersed in distilled water (125 mL), and next triethyl phosphate (18.2 g, 100.0 mmol) was added. The mixture was refluxed for 2 h, and this resulted in the formation of a stable dispersion. All volatiles were removed in vacuo, and a white powder (**A**) was obtained.

The synthesis of **B** was carried out according to the following procedure. Boehmite (2.0 g, 33.3 mmol) was dispersed in distilled water (50 mL), and next hydroquinone (0.1 g) and acrylic acid (4.8 g, 66.7 mmol) were added. The mixture was refluxed for 3 h, and this resulted in the formation of a stable dispersion. All volatiles were removed in vacuo, solid impurities were washed out by diethyl ether, and then a white powder (**B**) was obtained after drying.

Modification of the XSBL latex

The filler (**A** or **B**) was introduced into the latex in the form of an aqueous dispersion (10 wt %), and different amounts of the dispersions were applied to obtain the desired concentration of the modifier in the solid composite (from 0.5 to 4 wt %). The thus obtained systems were stirred for about 0.5 h at the ambient temperature to determine the exact modifier content for which the latex coagulation process occurred. The dispersions in which coagulation was not observed were examined by the dynamic light scattering method (DLS) and then were kept in flat glass vessels for 48 h at the ambient temperature. After that time, the water evaporated, and flexible, opaque films (0.4–0.5 mm thick) were obtained. The films of unmodified carboxylated styrene–butadiene rubber (XSBR) and modified carboxylated styrene–butadiene rubber (M-XSBR) containing 1, 2, or 3 wt % **A** or 0.5, 1, or 2 wt % **B** were used for further analysis.

For clarity, wt % without any further explanation is used whenever the modifier concentration regarding the solid phase of the composite (both in latex and in rubber) is concerned (in the main text, tables, etc.).

Rubber mixing

XSBR and M-XSBR master batches were prepared on a two-roll mill (friction ratio = 1 : 1.4, time of homogenization $\approx$ 10 min) according to PN-91 C-04258/1.

The compositions of the rubber mixtures are given in Table I.

Curing of the rubber mixtures

The vulcanization kinetic parameters for the different compounds were measured on a Monsanto MDR 2000 rheometer (Monsanto Chemical Co., Soda Springs, ID) at 165°C (measurement time = 0.5 h, oscil-

TABLE I
Compositions of the Rubber Mixtures

Constituent	System I			System II		
	I	A	B	II	IIA	IIB
LBSK 4148 (g)	100.0	—	—	100.0	—	—
LBSK 4148 + 1 wt % A (g)	—	100.0	—	—	100.0	—
LBSK 4148 + 1 wt % B (g)	—	—	100.0	—	—	100.0
ZnO (phr)	5.0	5.0	5.0	6.0	6.0	6.0
Stearic acid (phr)	2.0	2.0	2.0	1.0	1.0	1.0
Sulfur (phr)	—	—	—	1.0	1.0	1.0
CBS (phr)	—	—	—	3.5	3.5	3.5

phr = parts per hundred parts of rubber (by mass).

lation angle = 3°) according to PN ISO 289-1 : 1998/Ap1 : 1999. The values of the optimal vulcanization time (t_{90}) for the samples were determined.

The plate samples (145 mm × 145 mm × 2 mm) were vulcanized in a laboratory press at 165°C and a pressure of 200 kPa/cm^2 for t_{90} plus 5 min.

Characterization of the modifiers

The hydrogen and carbon contents were determined with a PerkinElmer CHNS/O II 2400 instrument (PerkinElmer, Inc., Waltham, MA). The aluminum content was determined as follows. The sample was mineralized to convert all aluminum atoms into the water-soluble form of Al^{3+}, the ions were then complexed with ethylenediaminetetraacetic acid (EDTA), and the excess of EDTA was titrated with an $FeCl_3$ solution.

Solid-state ^{27}Al magic-angle-spinning (MAS) NMR measurements were performed on a (Brucker DSX 300 spectrometer; Bruker BioSpin GmbH, Karlruhe, Germany) at a spinning rate of 6–10 kHz with proton high-power decoupling and a resonance frequency of 78.21 MHz with a recycle time of 0.5 or 1 s. Solid-state ^{13}C and ^{31}P cross-polarity/magic-angle-spinning NMR measurements were performed at spinning rates of 8.4 and 8 kHz and resonance frequencies of 75.47 and 121.50 MHz with recycle times of 6 and 1 s and contact times of 1.5 and 1.5 ms, respectively. Chemical shifts are reported with respect to external $[Al(H_2O)_6]^{3+}$ (^{27}Al), 85% H^3PO^4 (^{31}P), and tetramethylsilane (^{13}C and ^{1}H) standards.

Infrared spectra were collected on a Bio-Rad 165 Fourier transform infrared (FTIR) spectrophotometer (Bio-Rad Laboratories, Hercules, CA) with the samples in KBr pellets.

Particle size distribution

The particle size distributions in the aqueous dispersions were determined by the DLS method, and a Zetasizer Nano-ZS apparatus (Malvern Instruments, Ltd., Malvern, UK) was used.

Morphological characterization of the latex samples

Scanning electron microscopy (SEM) images of the powdered modifiers and rubber films were obtained on a Leo 1530 scanning electron microscope (LED Electron Microscopy Ltd., Cambridge, UK).

Mechanical tests for the latex and rubber samples

The mechanical properties of XSBR and M-XSBR films were measured on an Instron 5566 tensile testing machine at room temperature.

The Mooney viscosity measurements were carried out on a Mooney 2000E apparatus at 185°C according to PN-ISO 3417:98.

The tensile strength and elongation at break measurements were carried out on a Zwick 1445 apparatus according to ISO-37.

The tearing strength was measured on a Zwick 1445 apparatus according to PN-ISO 34–1:98.

The Shore hardness of the samples was measured on a Zwick Digital 7206-H04 apparatus (Zwick GmbH & Co., Ulm, Germany) according to PN-80/C-04 238.

RESULTS AND DISCUSSION

Synthesis and characterization of the fillers

Boehmite modified with diethyl phosphate (**A**) was prepared as discussed previously. The starting inorganic material, which consisted of spherical particles (diameter = 10–100 μm), was refluxed in an aqueous

TABLE II
Elemental Analysis of the Fillers

Modifier	Content (wt %)		
	C	H	Al
Boehmite[a]	—	1.7	45.0
A	5.1	2.5	31.5
B	24.9	3.0	22.6

[a] For the AlOOH formula.

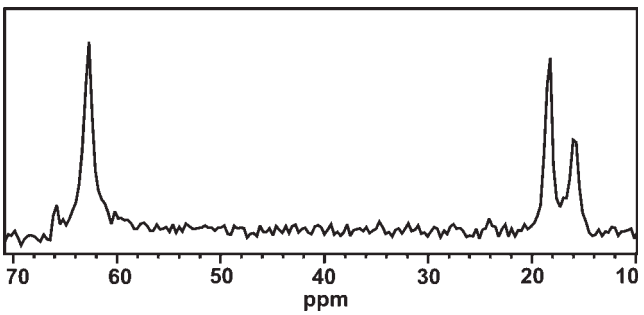

Figure 1 ^{13}C MAS NMR spectrum of **A**.

solution of triethyl phosphate. Under these conditions, triethyl phosphate underwent partial hydrolysis, yielding diethylphosphoric acid, which gradually destroyed the boehmite structure. As already mentioned, the reaction was stopped after 2 h. On the basis of the elemental analysis of **A** (Table II), it has been estimated that the product contains 16 wt % organic ligands, and the Al/P molar ratio is about 11.

^{13}C and ^{31}P MAS NMR spectra of **A** indicate that diethyl phosphate ligands exist in several different forms. The ^{13}C MAS NMR spectrum of **A** (Fig. 1) displays a broad signal for the methylene group (CH_2O: $\delta \approx 64$ ppm) and two distinctly separated resonances for the methyl groups (CH_3: $\delta \approx 16$ ppm and $\delta \approx 19$ ppm). The ^{31}P MAS NMR of **A** (Fig. 2) shows three signals at $\delta \approx -2$ ppm, $\delta \approx -7$ ppm, and $\delta \approx -15$ ppm. The latter resonance may be attributed to phosphate ligands bridging two aluminum atoms[18] [Al—O—P$(OC_2H_5)_2$O—Al], whereas the others are probably related to the monodentate or bidentate diethyl phosphate groups linked to a single Al atom. In the ^{27}Al MAS NMR spectrum of **A** [Fig. 3(b)], two resonances can be observed. A weak signal at $\delta \approx -26$ ppm indicates that A contains a small amount of the aluminum tris(diethylphosphate) phase [see eq. (2)], whereas the main signal at $\delta \approx -3$ ppm can be attributed to the AlO_6 octahedra in the boehmite structure.[16] The presence of the boehmite phase in **A** is confirmed by the FTIR

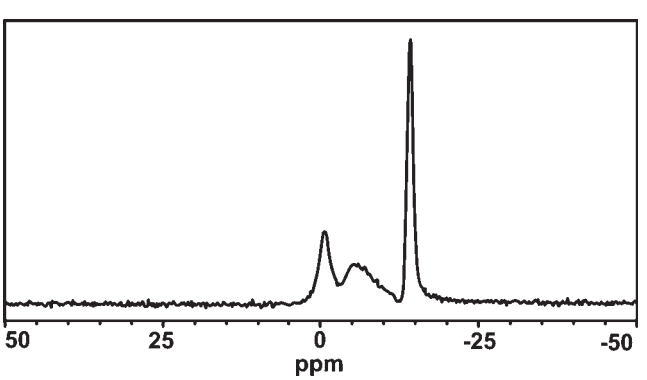

Figure 2 ^{31}P MAS NMR spectrum of **A**.

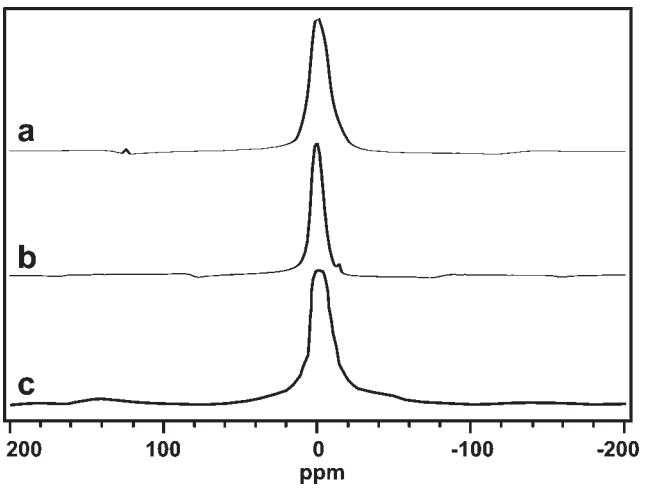

Figure 3 ^{27}Al MAS NMR spectra of (a) boehmite, (b) **A**, and (c) **B**.

spectrum [Fig. 4(b)], in which intensive signals typical for stretching vibrations in the distorted AlO_6 octahedron (ν at 484 and 613 cm^{-1}) as well as a group of bands characteristic of hydroxyl groups (ν_{as} at 3305 cm^{-1}, ν_s at 3072 cm^{-1}, δ_{as} at 1157 cm^{-1}, δ_s at 1072 cm^{-1}, and γ at 737 cm^{-1}) occur.

The reaction of boehmite and diethyl phosphate leads to the destruction of large primary boehmite agglomerates and results in the formation of a stable dispersion of nanoparticles. It consists of two populations of particles [Fig. 5(a); the average diameters measured by DLS are 40 and ca. 200 nm]; however, the fraction of smaller particles constitutes about 90% and about 100% of all particles by volume [Fig. 5(b)] and by number [Fig. 5(c)], respectively.

The elemental analysis of boehmite modified with acrylic acid (**B**) indicates that the average RCOO/Al molar ratio is equal to 0.83 (Table II). It cannot be

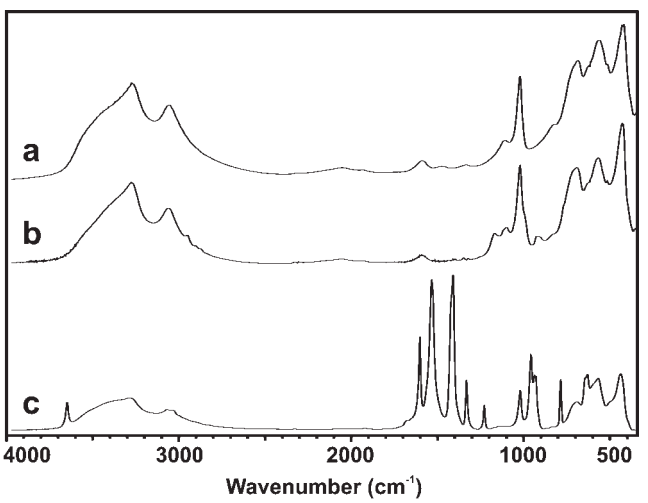

Figure 4 FTIR spectra of (a) boehmite, (b) **A**, and (c) **B**.

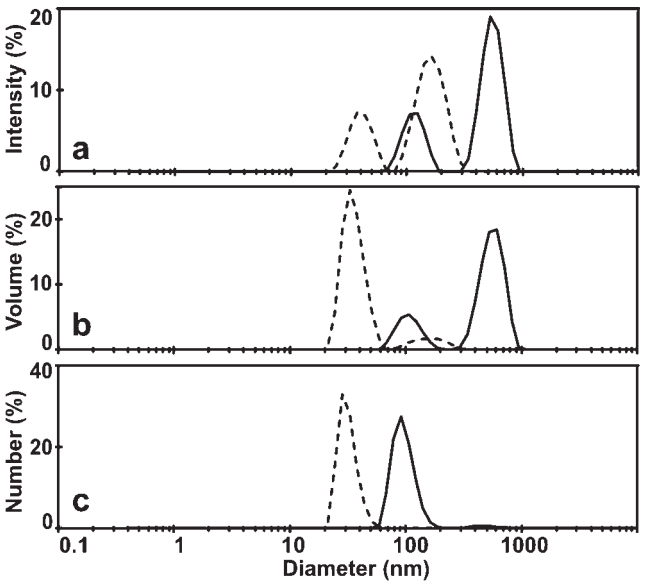

Figure 5 Particle size distribution of (- - -) A and (—) B by (a) intensity, (b) volume, and (c) number. Both products were dispersed in redistilled water (1 wt %).

excluded, however, that some **B** particles may have on their surface more than one organic ligand per Al atom.

Despite the high content of organic ligands, the absorption bands typical for boehmite are still present in the FTIR spectrum of **B** [Fig. 4(c)]. The most important bands related to organic ligands are at 1580 and 1457 cm^{-1} (ν_{as} and ν_s for bridging carboxylate anion), at 1007 and 980 cm^{-1} (γ for =CH bonds) and at 1648 cm^{-1} (ν for a C=C bond). The presence of unsaturated bonds is also confirmed by the ^{13}C MAS NMR spectrum of B (Fig. 6), in which a broad, strong signal at $\delta \approx 132$ ppm, typical for carbon nuclei in vinyl groups, can be observed. The spectrum also displays two resonances due to the carbon nuclei of carboxylate groups ($\delta \approx 170$ ppm and $\delta \approx 172$ ppm). The ^{27}Al MAS NMR spectrum of **B** [Fig. 3(c)] reveals, however, only one broad signal attributable to six-coordinate aluminum nuclei ($\delta \approx -5$ ppm). The absence of the bands typical for free carboxylic groups in the FTIR spectrum and the signals typical for chain aliphatic carbon nuclei in the ^{13}C MAS NMR spectrum indicates that acrylic

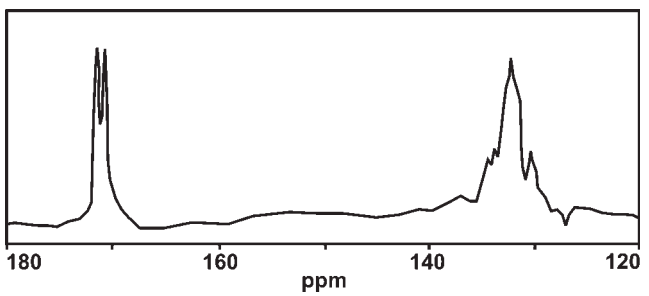

Figure 6 ^{13}C MAS NMR spectrum of **B**.

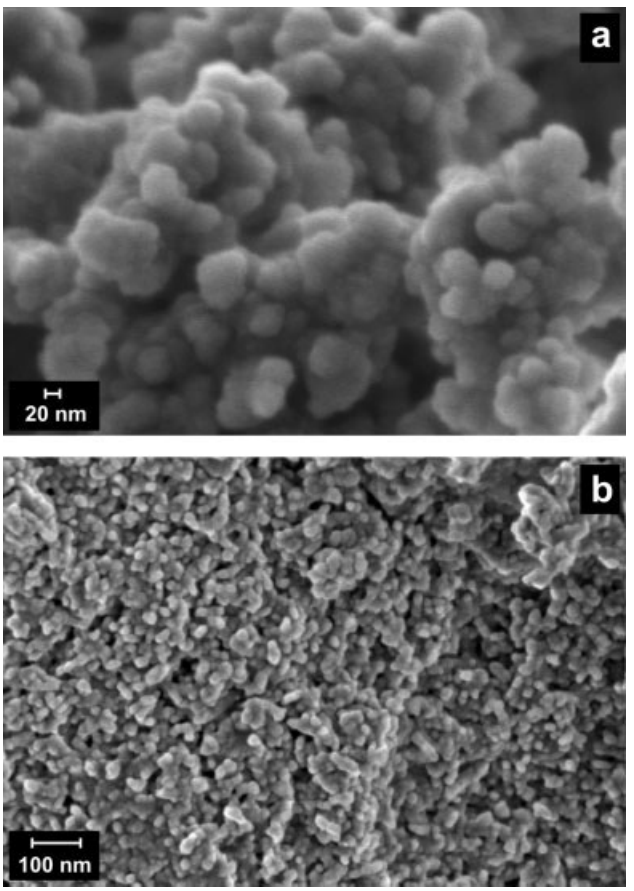

Figure 7 SEM images of (a) A (original magnification = 250,000×) and (b) B (original magnification = 100,000×).

acid homopolymerization does not occur during the synthesis of **B**.

B is easily dispersible in water, and the resulting dispersions contain two populations of particles [Fig. 5(a); the average diameters measured by DLS are 116 and 554 nm]. The fraction of smaller particles constitutes about 22% and about 98% of all particles by volume [Fig. 5(b)] and by number [Fig. 5(c)], respectively.

After the evaporation of water, the nanoparticles of **A** and **B** form large agglomerates that consist of

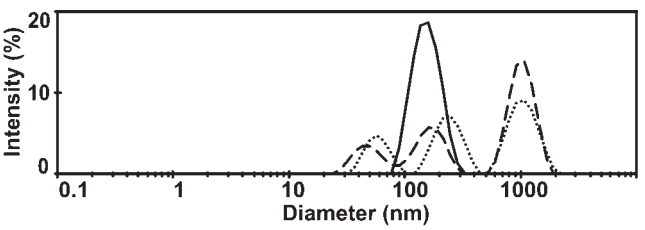

Figure 8 Particle size distribution by the intensity of (—) pure latex, (· · ·) latex modified with A (1 wt %), and (- - -) latex modified with B (1 wt %). The measurements were accomplished 0.5 h after the modifier incorporation.

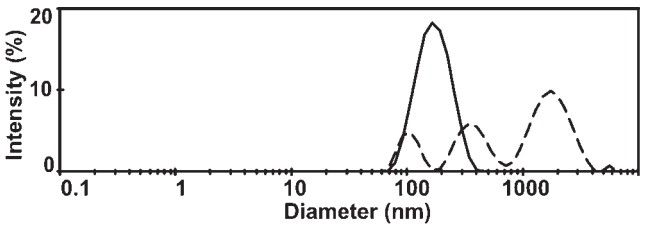

Figure 9 Particle size distribution by the intensity of (- - -) latex modified with B (1 wt %) 7 days after the modifier incorporation and (—) the same sample after dilution to about 10 wt % solids.

small spherical particles with an average particle size estimated from SEM to be less than 200 nm (Fig. 7).

Effect of the modification on the latex particle size

Commercially available XSBL shows a monomodal particle size distribution. The average diameter of the particles was determined by the DLS method under the assumption that the local viscosity of the medium in which the particles move is the same as that of water. For diluted latex dispersions of 0.5–1 wt %, the average size was found to be about 160 nm, whereas for commercial concentrated dispersions (ca. 48 wt %), the average size was still about 165 nm. The addition of aqueous dispersions of modifier **A** or **B** to commercial XSBL results in the agglomeration of some of the latex particles, whereas the diameter of the others decreases to less than 100 nm (Fig. 8). Unfortunately, a reliable quantitative analysis of these phenomena is not possible because of large differences between the measurement runs caused probably by the dynamic character of the agglomeration and disintegration processes. One may notice, however, that the tendency for agglomeration is much stronger in the case of the **B**-containing systems, and this tendency increases with an increase in the concentration of **B**. When the content of **B** was equal to 2.5 wt %, a permanent coagulation of XSBL occurred in a dozen or so minutes at room temperature. When the content of **B** was equal to 1 wt %, a slight increase in the latex particle size was observed in time. However, this process is reversible, and after dilution of the dispersion (to ca. 10 wt % of the solid phase), the particle size distribution is very similar to that of the unmodified latex (Fig. 9). In the case of the **A**-containing systems, the coagulation process runs more slowly, and stable dispersions containing up to 3 wt % **A** can be obtained (dispersions containing 4 wt % **A** coagulate after ca. 0.5 h).

The SEM image of the film prepared from the latex dispersion containing 3 wt % **A** [Fig. 10(a)] shows that the film is built up of rubber particles with an average diameter of about 20–30 μm. This may suggest that the concentration of the latex dispersions leads to gradual progress in coalescence. The film surface is homogeneous, and at a higher magnification, one cannot observe the modifier agglomerates [Fig. 10(b)]. Single particles (average diameter < 100 nm) can be seen in the fractures between nanospheres. However, a more precise analysis was impossible because of the degradation of the polymer matrix during the SEM study. Nevertheless, these observations point out that the latex concentration does not result in the agglomeration of the modifier nanoparticles, which are uniformly dispersed in the polymer matrix. The SEM image of the film prepared from the latex dispersion containing 2 wt % **B** [Fig. 10(c)] shows the presence of a fraction of small agglomerates (average diameter ≈ 5 μm), which indicates that the system is on the edge of coagulation. At a higher magnification, one can

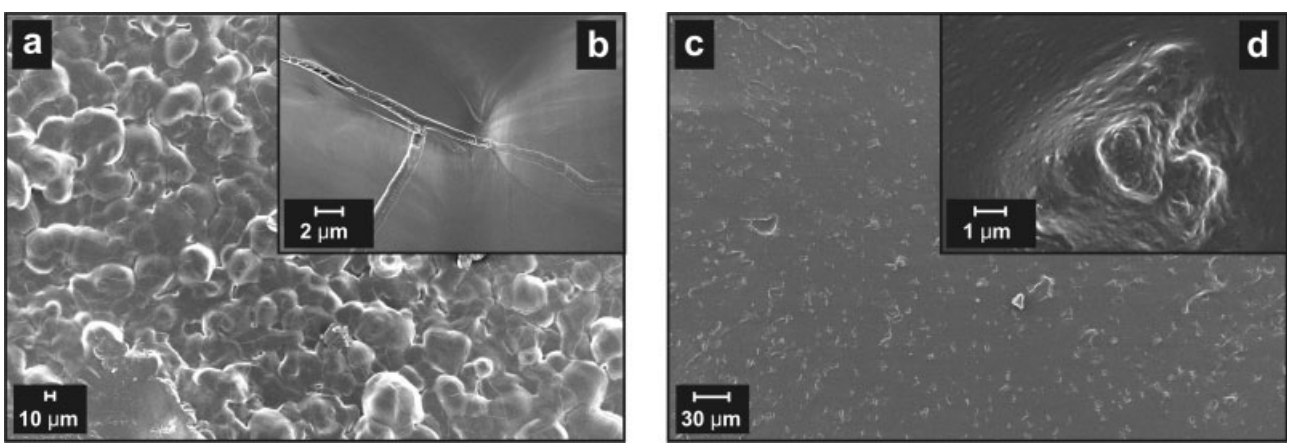

Figure 10 SEM images of M-XSBR modified with (a,b) A (3 wt %) and (c,d) B (2 wt %). The original magnifications were (a) 200, (b) 5000, (c) 500, and (d) 25,000×.

TABLE III
Effects of the Modification on the Rubber Viscosity and Solubility

Samples	Mooney viscosity (MU)[a]	Gel fraction (%)[b]
LBSK 4148	47.8	88.1
LBSK 4148 + 1 wt % **A**	42.0	88.2
LBSK 4148 + 3 wt % **A**	98.8	94.6
LBSK 4148 + 1 wt % **B**	39.0	90.8
LBSK 4148 + 2 wt % **B**	95.2	94.6

[a] At 185°C.
[b] After 48 h in toluene at room temperature.

observe that these agglomerates consist of both latex and modifier particles, and the remaining fraction of **B** particles (average diameter ≈ 150 nm) is homogeneously dispersed [Fig. 10(d)].

Rheological and mechanical properties of M-XSBR before vulcanization

The samples of unmodified rubber (XSBR) showed high values of the Mooney viscosity (ca. 48 MU at 185°C) because of the high content of the crosslinked chain fraction. Standard solubility tests indicate that a majority of the polymer phase (ca. 88%) is not soluble in toluene and forms a gel at room temperature. The Mooney viscosity of the composites (M-XSBR) containing 1 wt % **A** or **B** is distinctly lower than that of XSBR, whereas the gel-forming phase contents increase in an insignificant way (Table III). This means that for this concentration, the modifiers do not cause an increase in the rubber crosslinking index but work rather as plasticizers. A reverse phenomenon may be observed for M-XSBR containing 3 wt % **A** or 2 wt % **B**. The values of both the Mooney viscosity and gel fraction content for these systems are considerably higher than those of XSBR.

Mechanical tests for XSBR and M-XSBR films have proved that even small amounts of modifier **B** (0.5–2 wt %) cause a significant increase in the rubber stiffness. The growth of the **B** concentration in M-XSBR induces an increase in the Young's modulus (calculated for an elongation of 1%), the value of which for M-XSBR containing 2 wt % **B** is 40% higher than that in the case of unmodified rubber (Table IV). The stress necessary for a large elongation of the samples rises also in a monotonic way (e.g., the stress at 300% elongation increases by 26% in the case of M-XSBR containing 0.5 wt % **B** and by 126% in the case of M-XSBR containing 2 wt % **B**; Table V). The maximum tensile strength was observed for a sample containing 1 wt % **B**, and its value is about 200% higher than that in the case of XSBR, whereas the elongation at break of the same sample is higher by 45%. A sample containing 0.5 wt % **B** shows a similar value of the elongation at break, but the tensile strength is only 80% higher than that of XSBR (Table IV).

For the M-XSBR samples containing 1–2 wt % **A**, the values of the tensile strength and elongation at break increase by 10–20% only (Table IV).

At this stage of the work, it is hard to clearly explain why there are differences in the modifying efficiency between nanofillers **A** and **B**. One of the explanations is the fact that the **B** surface is more hydrophobic than that of **A** because of the much higher content of organic ligands (see Table II). Therefore, the strength of the polymer–filler interactions is probably higher in the systems doped with **B**, and this results in a stronger tendency toward coagulation in latices but also in much better mechanical properties of the composites obtained after the evaporation of water.

Rheological and mechanical properties of the vulcanized rubbers

The vulcanization of XSBR and M-XSBR containing 1 wt % **A** or **B** was carried out with two different curing systems: ZnO/stearic acid (system I) and ZnO/stearic acid/sulfur/CBS (system II; see Table I). In the case of system I, the curing process is based on the interactions between Zn^{2+} ions and carboxylic groups of the rubber, whereas in the case of system

TABLE IV
Mechanical Parameters of XSBR and M-XSBR Films

	Young's modulus[a]		Tensile strength		Elongation at break	
Sample	MPa	Δ (%)[b]	MPa	Δ (%)[b]	%	Δ[b] (%)
LBSK 4148	1.79	—	0.84	—	353.41	—
LBSK 4148 + 1 wt % **A**	2.16	21	1.00	19	398.09	13
LBSK 4148 + 2 wt % **A**	1.95	9	0.99	18	391.09	11
LBSK 4148 + 3 wt % **A**	2.66	49	1.05	25	350.05	−1
LBSK 4148 + 0.5 wt % **B**	2.21	23	1.52	81	532.93	51
LBSK 4148 + 1 wt % **B**	2.36	32	2.45	192	513.44	45
LBSK 4148 + 2 wt % **B**	2.52	41	2.41	187	457.96	30

[a] Calculated at an elongation of 1%.
[b] The Δ values were calculated with respect to the corresponding values for pure latex samples.

TABLE V
Stresses of XSBR and M-XSBR Films at Different Elongations

Sample	Stress at 100%		Stress at 200%		Stress at 300%	
	MPa	Δ (%)[a]	MPa	Δ (%)[a]	MPa	Δ (%)[a]
LBSK 4148	0.43	—	0.55	—	0.72	—
LBSK 4148 + 1 wt % **A**	0.50	16	0.62	13	0.77	7
LBSK 4148 + 2 wt % **A**	0.51	19	0.64	16	0.80	11
LBSK 4148 + 3 wt % **A**	0.57	32	0.73	33	0.93	29
LBSK 4148 + 0.5 wt % **B**	0.51	19	0.70	27	0.91	26
LBSK 4148 + 1 wt % **B**	0.60	40	0.91	65	1.29	79
LBSK 4148 + 2 wt % **B**	0.72	67	1.15	109	1.63	126

[a] The Δ values were calculated with respect to the corresponding values for pure latex samples.

II, unsaturated bonds of butadiene monomeric units participate in the crosslinking additionally. The mixtures containing system II display much higher Mooney viscosity, but the rheological tests show that the minimal values of torque after the prevulcanization step (M_{min}) for M-XSBR cured with both curing systems are very similar, and this suggests that their crosslinking indices are quite comparable (Table VI). The maximal values of the torque M_{max} for system I are more than 2 times lower than that for system II. This means that M-XSBR cured with system II shows much higher crosslinking density because of the formation of sulfur bridges. This way of crosslinking also supports the significant shortening of t_{90}. The presence of **A** or **B** in the case of system I also shortens t_{90}; therefore, it can be presumed that Al atoms form additional net points. In the case of system II, this effect is probably inessential, and the differences of t_{90} for XSBR and M-XSBR are inconsiderable (Table VI).

The influence of the modification on the four parameters describing the mechanical properties of vulcanized rubbers (tensile strength, elongation at break, tearing strength, and hardness) has been examined (Table VII). Generally, samples of vulcanized rubbers cured with system II show significantly higher tensile strength and slightly lower elasticity than rubbers cured with system I. The main reason for this is probably the difference in the crosslinking indices for these two systems. One may notice, however, that the addition of modifiers improves the tensile strength of rubbers independently of the curing system used. The highest increase in this parameter (ca. 40%) was observed for M-XSBR modified with **B** and cured with system II. For M-XSBR modified with **A**, a slightly better strengthening effect was observed (the tensile strength increased by ca. 35%) when system I was applied. The elongation at break of vulcanized rubbers increased insignificantly (2–18%) when the modifiers were added. The influence of the modifiers on the tearing strength depended on the sample preparation procedure. In the case of rubbers cured with system II, this parameter increased by 20–30%, whereas for the samples vulcanized with system I, a small increase in that for **B** and a small decrease in that for **A** were noticed. The influence of the modifiers on the Shore hardness of the vulcanized rubbers was negligible. For the samples cured with system I and system II, this parameter was equal to Shore A hardness values of 54–55 and 57–58°, respectively.

At this stage, it cannot be stated whether the described effects are due to the effective nanofiller–polymer interactions or due to the influence of the modifiers on the crosslinking process and the network structure. Both modifiers can be built into this network. There are Al—OH bonds on the surface of **A**, which may react upon heating with stearic acid and with carboxylic groups of XSBR. These reactions may lead to the formation of new net points and an increase in the hydrophobicity of **A** nanoparticles, which may be one of the reasons for

TABLE VI
Rheological Properties of the Rubber Mixtures

Parameter		Sample[a]					
		I	IA	IB	II	IIA	IIB
Rheometer	M_{max} (dN m)	3.76	3.85	3.83	8.89	8.77	8.72
	M_{min} (dN m)	2.62	2.38	2.07	2.34	2.39	2.23
	t_{90} (min : s)	15 : 50	13 : 38	10 : 49	4 : 40	4 : 58	4 : 51
Viscometer[b]	K (MU)	52.0	54.1	54.2	119.4	122.4	134.1

[a] The symbols are explained in Table I.
[b] The Mooney viscosity.

TABLE VII
Mechanical Properties of the Vulcanized Rubbers

	Tensile strength		Elongation at break		Tearing strength		Shore A hardness	
Sample[a]	MPa	Δ (%)[b]	%	Δ (%)[b]	kN/m	Δ (%)[b]	°	Δ (%)[b]
I	3.7	—	210	—	14.5	—	55	—
IA	5.0	35	243	16	12.3	−15	55	0
IB	4.8	30	219	4	16.1	11	54	−2
II	4.6	—	175	—	10.2	—	57	—
IIA	5.2	13	179	2	13.3	30	58	2
IIB	6.4	39	206	18	12.4	22	57	0

[a] The symbols are explained in Table I.
[b] The Δ values were calculated with respect to the corresponding values for pure rubber samples cured by the respective systems.

the tensile strength improvement in M-XSBR modified with **A** and cured with system I. On the other hand, there are unsaturated C=C bonds on the surface of **B** that may copolymerize with XSBR and sulfur if system II is applied. These two hypotheses must be, however, verified by further research, including a wider range of both rubbers and nanofillers, as well as more precise physicochemical analyses of the vulcanized composites.

CONCLUSIONS

In this work, it has been shown that stable aqueous dispersions of nanoparticles of boehmite modified with organic ligands may be obtained in very simple reactions between γ-AlOOH and inexpensive reagents such as triethyl phosphate or acrylic acid. Nanoparticles in this form can be easily incorporated into XSBL (LBSK 4148). DLS analyses show that hybrid nanoparticles may cause agglomeration of the latex particles. Above a certain critical concentration of the nanofiller, irreversible latex coagulation occurs. When the modifier concentration is below a threshold value (2–3 wt %, dependent on the type of modifier used), systems are obtained that after water evaporation afford films, in which the nanoparticles are homogeneously dispersed. Even such small amounts of modifiers (especially of **B**) are sufficient for substantial improvements in the mechanical properties of rubbers. In some systems, the tensile strength and elongation at break increase by about 200 and 40%, respectively. It seems that after appropriate optimization of the modifier structure, such composites could be used in technologies in which latices are usually applied as gaskets or high-elasticity binder agents. The mechanism on how these modifiers change the latex properties is unknown. One of the possibilities is that intermolecular interactions between the surfactant (coating latex particles) and modifier occur. This results in transient crosslinking that stiffens the composite but may decline under the stress.

The addition of nanofillers can also improve some of the mechanical properties of vulcanized rubbers. It seems, however, that this kind of modification is useless for the examined systems because of the too high viscosity of the latex used (LBSK 4148) and poor mechanical properties of the vulcanized rubbers. Therefore, we plan to carry out a similar cycle of experiments for other types of latices (e.g., latex of natural rubber).

The authors would like to thank Dr. Jeffrey Fenton and CONDEA-Vista Co. for complimentary delivery of boehmite samples.

References

1. Lagaly, G. Solid State Ionics 1986, 22, 43.
2. Vaia, R. A.; Teukolsky, R. K.; Giannelis, E. P. Chem Mater 1994, 6, 1017.
3. Vaia, R. A.; Giannelis, E. P. Macromolecules 1997, 30, 800.
4. Reichert, P.; Kressler, J.; Thomann, R.; Mülhaupt, R.; Stöppelman, G. Acta Polym 1998, 49, 116.
5. Weimer, M.; Chen, H.; Giannelis, E. P.; Sogah, D. Y. J Am Chem Soc 1999, 121, 1615.
6. Hawker, C. J.; Bosman, A. W.; Harth, E. Chem Rev 2001 2001, 101, 3661.
7. Fisher, H. Mater Sci Eng C 2003, 23, 763.
8. Leroux, F.; Besse, J. Chem Mater 2001, 13, 3507.
9. Apblett, A. W.; Warren, A. C.; Barron, A. R. Chem Mater 1992, 4, 167.
10. Apblett, A. W.; Landry, C. C.; Mason, M. R.; Barron, A. R. Mater Res Soc Symp Proc 1992, 249, 75.
11. Landry, C. C.; Pappé, N.; Mason, M. R.; Apblett, A. W.; Tyler, A. N.; MacInnes, A. N.; Barron, A. R. J Mater Chem 1995, 5, 331.
12. Callender, R. L.; Harlan, C. J.; Shapiro, N. M.; Jones, C. D.; Callahan, D. L.; Wiesner, M. R.; MacQueen, D. B.; Cook, R.; Barron, A. R. Chem Mater 1997, 9, 2418.
13. Landry, C. C.; Pappé, N.; Mason, M. R.; Apblett, A. W.; Barron, A. R. Inorganic and Organometallic Polymers; ACS Symposium Series 572: Washington, DC, 1994, II, p 149.
14. Vogelson, C. L.; Koide, Y.; Alemany, L. B.; Barron, A. R. Chem Mater 2000, 12, 795.
15. Florjańczyk, Z.; Lasota, A.; Wolak, A.; Zachara, J. Chem Mater 2006, 18, 1995.
16. Florjańczyk, Z. Wolak, A.; Dębowski, M.; Plichta, A.; Ryszkowska, J.; Zachara, J.; Ostrowski, A.; Jurczyk-Kowalska, M. To be submitted.
17. Zygadło-Monikowska, E.; Florjańczyk, Z.; Wolak, A.; Lasota, A.; Plichta, A. Pol. Pat. 368877 (2006).
18. Chakraborty, D.; Horchler, S.; Krätzner, R.; Varkey, S. P.; Pinkas, J.; Roesky, H. W.; Usón, I.; Noltemeyer, M.; Schmidt, H.-G. Inorg Chem 2001, 40, 2620.